

NAVIGATION GRADE MEMS ACCELEROMETER

Pascal Zwahlen¹, Anne-Marie Nguyen¹, Yufeng Dong¹, Felix Rudolf¹, Marc Pastre², Hanspeter Schmid³

¹Colibrys S.A., ²EPFL, ³FHNW

ABSTRACT

This paper reports on a high performance navigation grade MEMS servo accelerometer targeted at inertial applications. Reported results are for a bulk MEMS capacitive sensor with 11g full scale over a 300 Hz bandwidth interfaced with a highly optimized servo-loop 5th-order sigma-delta electronic. Measurements demonstrate a long-term bias stability of +/-0.2mg, a second order non-linearity $K_2 < 5 \mu\text{g}/\text{g}^2$, an in-band noise floor of $1 \mu\text{g}/\sqrt{\text{Hz}}$ and a Dynamic Range over 1 Hz bandwidth of 22 bits.

INTRODUCTION

Inertial high performance accelerometer market can be segmented into several categories: tactical grade, navigation grade and military grade each characterized by an order of magnitude improvement on bias stability, linearity and noise.

Penetrating the inertial navigation grade market faces competition from established technologies like macro electro-mechanical servo accelerometers [1] and quartz resonating accelerometers [2]. While the macro electro-mechanical accelerometers reach high performances, they are expensive and fragile [3]. On the other hand quartz resonators have excellent dynamic range but exhibit degraded stability performance and very low g shock tolerance.

MEMS have the potential of low-cost high volume production thanks to its batch processing manufacturing. It can also be made very high g shock tolerant, without post-shock performance degradation. Mid to high performance open-loop MEMS accelerometer are today commercially available and reach tactical grade performances with stability of 1.5 mg or 150 ppm, total harmonic distortion of 50dB and an SNR of 97 dB[4]. Ultimate evolution of the open-loop MEMS sensor is seen at a stability of 100 ppm, a THD of 60 dB and an SNR of 140 dB [3]. Bringing MEMS accelerometer one step further towards higher performance navigation grade, requires operating the MEMS accelerometer in a servo mode.

MEMS servo accelerometers have already demonstrated high performance in low g applications for earthquake monitoring or geoseismic imaging. Noise floor as low as $-145 \text{ dBg}/\sqrt{\text{Hz}}$, with a working range of $\pm 0.3\text{g}$ including 1g gravity compensation have already been reported [5]. The challenge to bring this technology towards inertial navigation is about significantly improving the bias stability. Compared to

other previously reported works [6], [7], this design takes advantage of the extremely good mechanical characteristics of the sensor allowing for relaxed requirements on the electronics side. Sensor mechanical bias stability has been demonstrated to be a key contributor to the overall bias stability budget even in servo-loop operation.

Previous publication [8] detailed the design of a generic sigma-delta electronic with a versatile analog front-end allowing a broad range of capacitive accelerometers to be interfaced. The present work reports on measured performances (stability, non-linearity, noise, dynamic range, shock and, temperature coefficients) and compares them against simulated and analytical models.

SYSTEM DESIGN

Servo loop architecture

Different servo loop configurations have been evaluated. Sigma-Delta pulse modulation principle has been chosen over analog feedback schemes (voltage amplitude modulation) because of its improved linearization of the electrostatic forces, resulting in superior system non-linearity performance. The chosen architecture is illustrated in figure 1 and further detailed in [8].

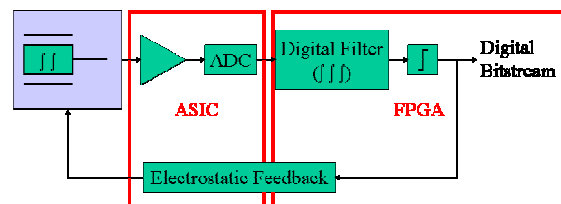


Figure 1 : Schematic of servo-loop system with ADC multi-bit quantizer noise shaped by the mechanical integrators and the 1-bit comparator shaped by the 3rd order digital filter.

The position of the proof mass is measured with a capacitive analog front-end amplifier followed by a low resolution A/D converter. Further loop filtering, which aims at rejecting noise in high frequency band, is thus performed in digital domain and hardware implemented in a FPGA. Finally a 1-bit comparator defines the sign of the signal, which is the output bitstream, and determines the direction in which the actuation force is applied to the sensor. This depicted architecture has the following advantages:

- System high resolution comes from the oversampling technique of the Sigma-delta

operation and the 5th order noise shaping implementation. In consequence low resolution on the signal read-out is sufficient, thus significantly relaxing the constraints on the analog electronic design.

- System versatility is given through digital loop filtering. Thus bandwidth, working range and noise can easily be tailored to the specific end application requirements.

All this comes however at the expense of increased system design complexity because of the non-linear characteristics of the 1-bit comparator. Simple linear system modelization is no more possible, requiring extensive numerical simulation analysis performed on a Simulink platform.

The main system design focuses, in order to achieve the high performance required for inertial navigation grade accelerometer, are non-linearity, noise and stability.

From the already very linear characteristic of the sigma-delta loop, further tuning of the mass median position has been implemented such as to better symmetrise the electrostatic pull-up and pull-down actuation force.

Complete system noise analysis has been performed accounting for all the major noise sources described in [9]:

- Mechanical Brownian noise could be reduced by operating the MEMS sensor at high quality factor. Seismic mass damping is achieved by electrostatic feedback actuation. In this reported article Brownian noise has been set at $0.4 \mu\text{g}/\sqrt{\text{Hz}}$, but not limited by the technology as values as low as $0.03 \mu\text{g}/\sqrt{\text{Hz}}$ have been achieved [3].
- To minimize the effect of the front-end amplifier noise, the sensor gain has to be maximized, thus designing for small mechanical spring, large capacitance area and small gap.
- Voltage reference noise and $1/f$ noise have been rejected using standard correlated double sampling techniques.
- Quantization noise and mass residual motion can be made small providing proper choice of system sampling frequency. For this reported 11g sensor, sampling frequency has been set at 685 kHz.

The third key design focus mentioned is bias stability (offset). Major improvements have been reached on the mechanics side through careful MEMS design of the springs and their anchoring, process flow adjustments to make the MEMS more rigid and proper assembly stress decoupling techniques. Operating the system in a servo-loop configuration allows for further electronics induced bias drift rejection by smart choice of the actuation voltage. On the other hand, close-loop operation introduces additional bias drift error coming from the stability of the voltage supply used for actuation. However, this source of drift can be made

small with careful selection of voltage references ($<50 \text{ ppm}$). Overall bias stability then becomes dominated by mechanical stability is estimated to be below 5 pm of mass displacement variation.

MEMS Sensor design

The choice of the optimal MEMS technology and design determines largely the ultimate performance of the sensor. The driving factors for this application are:

- Low vacuum combined with large mass for high quality factor and low Brownian noise.
- Rigid and stable structure for low mechanical bias stability.
- Good manufacturing tolerance capability in order to keep electronic input referred noise at low value.
- Reasonably large capacitive surfaces and small gaps in order to generate enough actuation forces without increasing too much the actuation voltage ($<30 \text{ V}$) and consequently the power consumption.
- Robustness in order to withstand high shock and vibrations.

Based on these requirements the best candidate is an out-of-plane capacitor structure as illustrated in figure 2. The bulk through-silicon wafer micromachining allows large mass, large capacitive area and an overall rigid structure. Good manufacturing tolerance is achieved by DRIE etching of the seismic mass. The 3-stack wafer assembly is performed using silicon fusion bonding technique achieving very good hermeticity, low vacuum levels of typically 0.3 mbar and a good control over the inter-electrode gap. By targeting this gap at a low value of about $2 \mu\text{m}$ high shock tolerance of above 4000g is achieved.

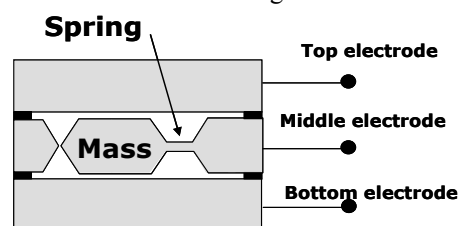


Figure 2 : Generic out-of-plane capacitive MEMS sensor.

TEST RESULTS

Noise & Dynamic performance

Noise measurements have been performed in a quiet room taking special care with additional ground mechanical decoupling, making it suitable for noise measurements down to $30\text{ng}/\sqrt{\text{Hz}}$. Typical noise curves show a noise value in the 300 Hz

baseband of $1.7\mu\text{g}/\sqrt{\text{Hz}}$ or below (figure 3) in excellent accordance with Simulink simulations.

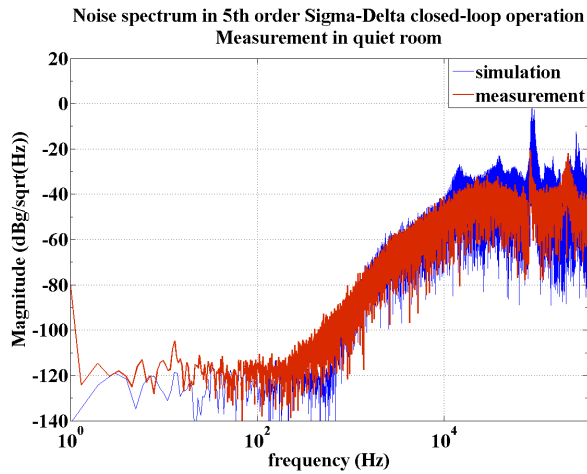


Figure 3 : Noise spectrum showing a bandwidth of 300 Hz with excellent matching between measurements and simulations.

Dynamic measurements on a shaker, with an additional 1g static load (figure 4), show a max sine acceleration of 10.7g, resulting in a total DR of 22.2 bits in a 1Hz bandwidth or 18.1 bits in a 300 Hz bandwidth. Low frequency noise hump has been demonstrated to be linked with building environmental noise. This hump disappears when taking special care for noise decoupling structure as in figure 3. Harmonics seen on figure 4 are not linked to system non-linearity but solely due to shaker non-linearity as was verified by attaching a highly linear piezo-electric reference sensor on top of the measured device.

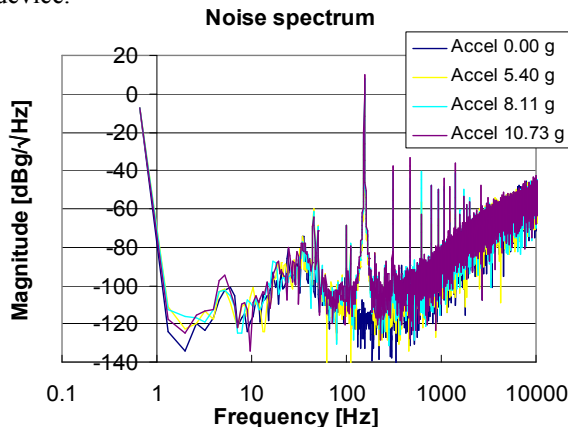


Figure 4 : Dynamic measurements. Excitation signal of 1g static + sine excitation at 155 Hz at multiple amplitudes.

Bias stability

Long term bias stability measurements (figure 5) have demonstrated overall values of ± 0.2 mg or 20 ppm without compensating for voltage actuation drift. The lab voltage supply used for this measurement presents a stability of 200 ppm, resulting in 0.15 mg stability after some theoretical calculation (model partially

validated by measurements). The purely mechanical bias stability is expected to be at ± 0.05 mg or ± 5 ppm.

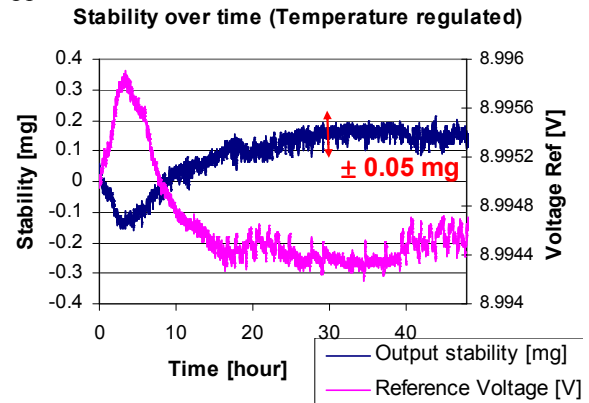


Figure 5 : Stability measurement over time at regulated temperature. Initial stability variation is due to voltage reference instability.

Working with standard of the shelf voltage reference supplies of 50 ppm, overall stability of less than ± 0.1 mg or ± 10 ppm is expected.

Non-linearity K2

Bias shift induced by vibration and shifted to DC through sensor non-linearity (dominated by second harmonic K2), called vibration rectification error (VRE) is an important parameter for inertial navigation. Extremely low K2 non-linearity value $< 10 \mu\text{g}/\text{g}^2$ are reported in figure 6. However, due to the servo-loop operation and excellent linearization capability of the electrostatic forces through sigma-delta control, K2 is expected to be below $1 \mu\text{g}/\text{g}^2$. Reported values are still limited by measurement capabilities and not system performance. Identified error sources (open-loop servo shaker, noise from the high power electro-magnetic motor, shaker distortion) have been evaluated and reported as error bars in figure 6.

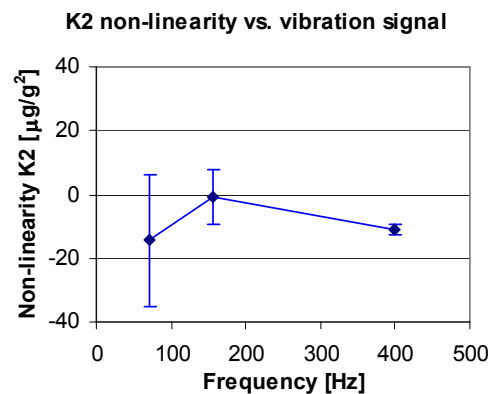


Figure 6 : K2 non-linearity as a function of signal frequency vibration. Excitation amplitude is set at 2g peak. Theoretical error bars are also provided.

Temperature performance

Preliminary temperature characterizations from -30°C to +80°C window show a temperature bias as low as 100µg/°C, and a typical K1 scale factor <75 ppm/°C.

Performance summary

Table 1 reviews the list of the reported performances and compares them with the industry standard, the Honeywell Q-Flex 2000-030 [1].

Table 1 : Performance review

	Colibrys	QA 2030	Unit
Input range	11.7	60	g
Noise	1.7	3	µg/√Hz
Dynamic range (1Hz BW)	22.2	24.2	bits
Bandwidth	400	500	Hz
Bias stability (24 hrs)	0.1	0.1	mg
Non-linearity K2	<10	<20	µg/g ²
Bias temperature coefficient	100	<30	µg/°C
Scale Factor temp. coefficient	75	180	ppm/°C

CONCLUSIONS

Measurements show that MEMS accelerometers match performance of expensive macro electro-mechanical sensors such as the QA2000 [1] and even outperform them significantly in noise, linearity (VRE), robustness and cost. After having conquered the automotive and consumer markets, MEMS accelerometer are getting ready for the most demanding applications replacing advantageously the rugged electro-mechanical devices.

ACKNOWLEDGMENT

The authors wish to thank the Swiss CTI for financial support of this project.

REFERENCES

[1] Honeywell, QA2000 Q-Flex® Accelerometer, <http://www.inertialsensor.com/qa2000.shtml>
 [2] Innalabs Quartz Accelerometers Datasheet, [www.innalabs.com/datasheets/accelerometers/Innalabs_Accel_INN-201\(202\)_Oct2009.pdf](http://www.innalabs.com/datasheets/accelerometers/Innalabs_Accel_INN-201(202)_Oct2009.pdf)
 [3] F. Rudolf, P. Zwahlen, Y. Dong, "MEMS accelerometers for highest performance applications" 9th SEGJ International Symposium
 [4] Colibrys Accelerometer RS9010 Datasheet, <http://www.colibrys.com/e/page/300/>

[5] J. Gannon, H. Pham, K. Speller, "A Robust Low Noise MEMS Accelerometer" Proc. of the ISA Emerging Technologies Conference, Houston, TX, Sept. 10-12, 2001.
 [6] J.M. Tsai, G.K. Fedder, "Mechanical Noise-Limited CMOS-MEMS Accelerometers" Tech. Digest MEMS 2005, Miami Beach, pp. 630-633
 [7] M. Lemkin, B.E. Boser, "A Three-Axis Micromachined Accelerometer with a CMOS Position-Sense Interface and Digital Offset-Trim Electronics" IEEE J. of Solid-State Circuits, Vol. 34, No. 4, pp. 456-468, April 1999
 [8] M. Pastre, M. Kayal, H. Schmid, A. Huber, P. Zwahlen, A.-M. Nguyen, Y. Dong, "A 300 Hz 19b DR Capacitive Accelerometer based on a Versatile Front End in a 5th-order Delta-Sigma Loop", ESSCIRC, Athens, Greece, Sept. 14-18, 2009
 [9] H. Kùlah, J. Chae, N. Yazdi, K. Najafi, "Noise Analysis and Characterization of a Sigma-Delta Capacitive Microaccelerometer" IEEE J. of Solid-State Circuits, Vol. 41, No. 2, pp. 352-360, February 2006